© 2023. Published by The Company of Biologists Ltd | Journal of Experimental Biology (2023) 226, jeb245063. doi:10.1242/jeb.245063

RESEARCH ARTICLE

Hawkmoths regulate flight torques with their abdomen for yaw control

Viet Le[1], Benjamin Cellini[1,*], Rudolf Schilder[2] and Jean-Michel Mongeau[1,‡]

ABSTRACT

Many animals use body parts such as tails to stabilize posture while moving at high speed. In flying insects, leg or abdominal inertia can influence flight posture. In the hawkmoth *Manduca sexta*, the abdomen contributes ∼50% of the total body weight and it can therefore serve to inertially redirect flight forces. How do torques generated by the wings and abdomen interact for flight control? We studied the yaw optomotor response of *M. sexta* by using a torque sensor attached to their thorax. In response to yaw visual motion, the abdomen moved antiphase with the stimulus, head and total torque. By studying moths with ablated wings and a fixed abdomen, we resolved abdomen and wing torques and revealed their individual contribution to total yaw torque production. Frequency-domain analysis revealed that the abdomen torque is overall smaller than wing torque, although the abdomen torque is ∼80% of the wing torque at higher visual stimulus temporal frequency. Experimental data and modeling revealed that the wing and abdomen torque are transmitted linearly to the thorax. By modeling the thorax and abdomen as a two-link system, we show that abdomen flexion can inertially redirect the thorax to add constructively to wing steering efforts. Our work argues for considering the role of the abdomen in tethered insect flight experiments that use force/torque sensors. Taken together, the hawkmoth abdomen can regulate wing torques in free flight, which could modulate flight trajectories and increase maneuverability.

KEY WORDS: Insect flight, Inertial redirection, *Manduca sexta*, Optomotor response

INTRODUCTION

Controlling and sustaining flight in animals is a complex task that requires coordination of sensors and actuators. In flapping-wing flight – the dominant mode of aerial locomotion in nature – the wings produce lift and thrust that allows animals to translate in the air. Wing–air interactions allow the wings to produce the necessary forces to hover and to maneuver the body (Sane, 2003). Many studies of insect flight have therefore focused on these forces generated by the wings. However, flying, running and leaping animals can use body parts to rapidly redirect inertial forces. For instance, gliding geckos use their tails to turn (Jusufi et al., 2008), falling squirrels use their tails for aerial righting (Fukushima et al., 2021), leaping lizards use their tails to control pitch (Libby et al., 2012), sprinting cheetahs swing their tails for balancing (Shield et al., 2021), hawkmoths can use their abdomens for pitch regulation (Dyhr et al., 2013), beetles move their legs to regulate yaw torque (Li et al., 2017), and the legs and abdomen of fruit flies can fine-tune posture in flight (Berthé and Lehmann, 2015). Movement of body parts such as the tail or abdomen could increase agility and stability during rapid maneuvers by redirecting inertia.

In insects, the abdomen, owing to its typically large mass and inertia relative to those of the legs, could play an important role in flight control. During the optomotor response, fruit flies (Götz et al., 1979; Zanker, 1988), locusts (Camhi, 1970a,b) and moths (Dyhr et al., 2013; Parthasarathy and Willis, 2018) move their abdomen. Prior studies in hawkmoths suggested that the abdomen could act as a brake in reducing the yaw torque generated by the wings (Hedrick and Daniel, 2006; Hinterwirth and Daniel, 2010; Parthasarathy and Willis, 2018). However, it has not been demonstrated explicitly to what extent the abdomen could regulate wing-generated torques and, therefore, overall torque production in flight.

To determine the extent to which hawkmoths can modulate flight forces with their abdomen, we studied the yaw optomotor response using a torque sensor fixed to the thorax. During the optomotor response, we confirmed that moths generated a torque in phase with the visual stimulus, but that the abdomen moved out of phase. To resolve the role of the abdomen and wings, we measured yaw torques of wingless and abdomen-fixed moths. By combining frequency-domain analysis and numerical simulation, we show that the moth abdomen can regulate wing torques and can constructively influence overall yaw torque production in flight.

MATERIALS AND METHODS

Animal

Manduca sexta (Linnaeus 1763) hawkmoths were reared in the Department of Entomology at The Pennsylvania State University. Caterpillars and moths were kept under 16 h:8 h light:dark, 25°C ambient temperature and 55% relative humidity. Moths of both sexes aged 3 and 5 days post eclosion were used in experiments. Moths were fed a standard *M. sexta* artificial diet with an agar base (Frontier Scientific, F9783B).

Experimental setup

The flight paradigm was designed to measure torque responses produced by the hawkmoth *M. sexta* while perturbed by a translatory visual stimulus (Fig. 1A,B). Moths were tethered to a factory-calibrated six-axis force/torque sensor (Nano17 Titanium, ATI Industrial Automation) using a custom 3D-printed mount. The sensor provided a torque resolution of 0.0069 N mm and a range of 50 N mm. The moth tether end was beveled at 40 deg to reproduce the natural flying pitch angle of hawkmoths (Hedrick and Daniel, 2006). We used a 27-inch LCD monitor with a 144-Hz refresh rate

[1]Department of Mechanical Engineering, The Pennsylvania State University, University Park, PA 16082, USA. [2]Departments of Biology and Entomology, The Pennsylvania State University, University Park, PA 16082, USA.
*Present address: Department of Mechanical Engineering, University of Nevada, Reno, NV, USA.

‡Author for correspondence (jmmongeau@psu.edu)

B.C., 0000-0002-0609-7662; R.S., 0000-0003-1229-1274; J.-M.M., 0000-0002-3292-6911

Received 15 September 2022; Accepted 17 March 2023

Journal of Experimental Biology (2023) 226, jeb245063. doi:10.1242/jeb.245063

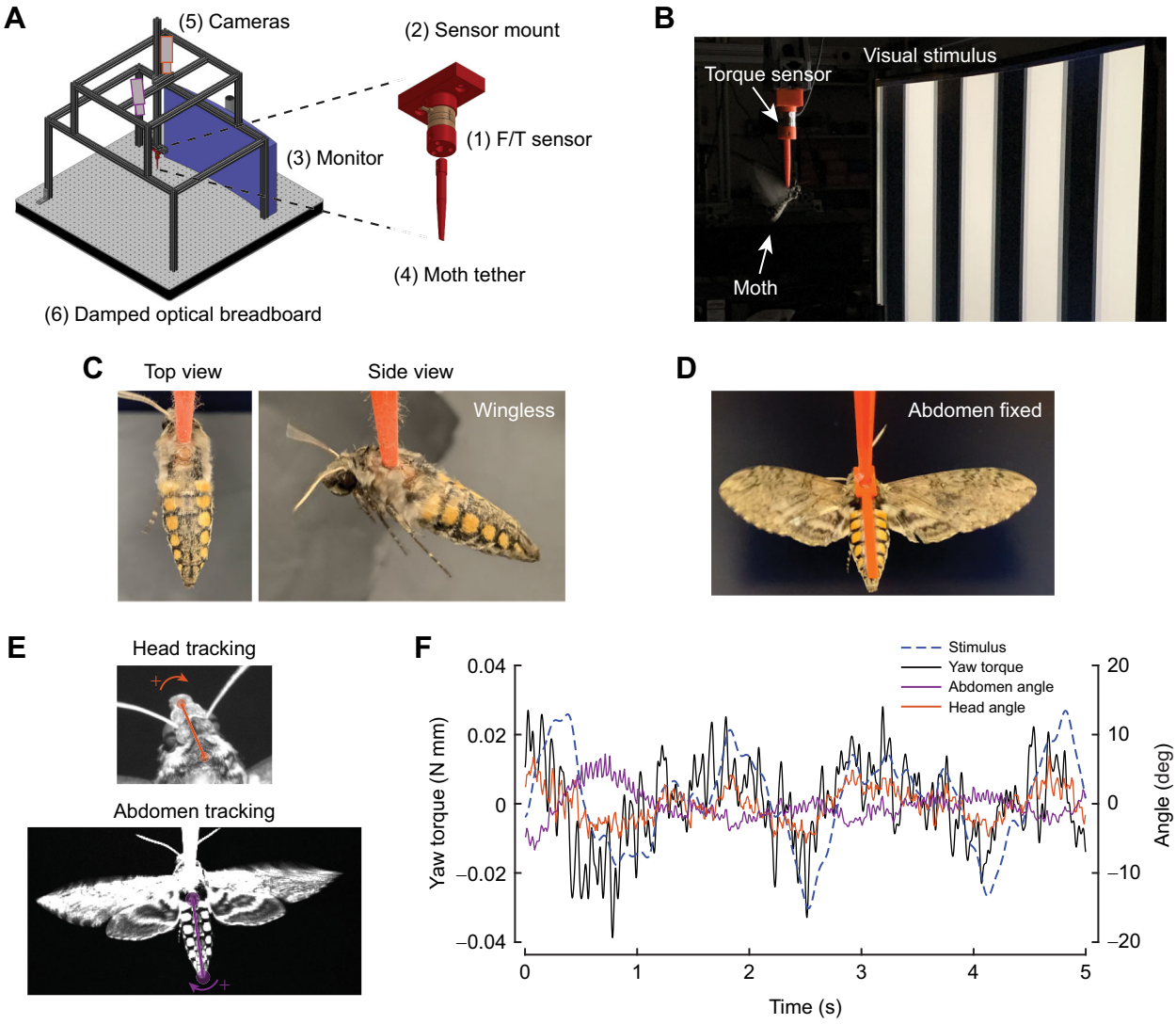

Fig. 1. Experimental setup and methods. (A) Force/torque (F/T) sensor (1) attached to a custom 3D-printed mount (2) positioned in front of a computer monitor (3) displaying the stimulus. The moth was attached to a custom, 3D-printed tether (4) and filmed with two overhead cameras (5). The experimental rig was mounted to a damped optical breadboard (6) to reduce external vibration. (B) Side view of an experimental trial. (C) Top and side view of a tethered, wingless moth. (D) Abdomen-fixed moth attached to a custom 3D-printed rod. (E) Single frame of head and abdomen tracking using image processing. Arrows represent the clockwise positive global coordinate system. (F) A representative trial of the moth yaw optomotor response.

(27HC1R Pbidpx, AOPEN) to display visual stimuli to stimulate the moth visual system (Fig. 1B). The framing and monitor were mounted on an optical breadboard to damp external vibrations. The brightness of the screen was adjusted to 30% of its maximum brightness (75 cd m^{-2}), which is near the peak optomotor response for *M. sexta* (Parthasarathy and Willis, 2018).

Stimulus

To generate an optomotor response, we presented moths with a wide-field visual stimulus with a spatial wavelength of 20 deg. The stimulus motion was prescribed by a sum-of-sines signal consisting of five frequency components (0.65, 1.15, 2.0, 3.6 and 6.35 Hz) that were logarithmically spaced and chosen to avoid interference from harmonics (Roth et al., 2011) (Fig. S1A,B). Furthermore, each sine component had a randomized phase. Unlike a linear-time-invariant system in which the response will be a function of frequency alone, insect visual systems, including individual neurons (Eckert, 1980), are sensitive to the velocity of visual stimuli (Hassenstein and Reichardt, 1956). Therefore, as we have done previously, we normalized the angular velocity of each sine component by scaling the amplitude (A) according to $A = \dot{\theta}_{norm}/2\pi f$, where f is the frequency and $\dot{\theta}_{norm}$ is the normalized angular velocity (Cellini and Mongeau, 2020; Cellini et al., 2022). The visual stimulus was normalized to a velocity of 30 deg s^{-1} (Fig. S1B), which is near the optimal response of wide-field motion detecting neurons in *M. sexta* (Theobald et al., 2010) and peak steady-state responses of *M. sexta* elementary motion detector output (Windsor and Taylor, 2017). Furthermore, we constrained the stimulus to a peak-to-peak A of ∼20 deg to avoid saturation (nonlinearities) of the head about yaw (Fig. S1B).

Experimental procedure

Moths were placed on ice for 20 min to induce anesthesia. Moths were kept cold during the tethering process using a Peltier stage held at approximately 4°C. Scales on the thorax were removed before placing moths on a custom holder, which consisted of a rectangular

aluminium plate with a cut-out slot for the moth. The moth thorax was sanded gently to create a rough surface before affixing the tether with cyanoacrylate glue (Ultra Gel Control, Loctite Super Glue). After the moths were tethered, they were allowed to acclimate to the lab environment (dark surroundings at 23°C) for 30 min before starting experimental trials. Three types of experiments were performed, which we detail below.

Intact moths

After warming up, moths were shown the stimulus. There were no restrictions to the wings and abdomen.

Wingless experiment

Moths were cooled down for an extra 10 min to ensure that they were fully immobilized during the surgery. Moths were placed on the Peltier stage with their wings spread out. Before ablation, the wings were fixed to the tether. Large portions of the wings (∼98% of total area) were ablated with the wing stem left intact (Fig. 1C).

Abdomen-fixed experiment

The moth abdomen was affixed to a 3D-printed rod (acrylonitrile butadiene styrene or ABS) along the length of the abdomen (Fig. 1D). The rod was fixed to the tether rod such that abdomen torques were transmitted internally through the rod and not the torque transducer.

Intact moths used for analysis had a minimum of three 20-s trials with continuous flight. To ensure robust yaw compensation, we only accepted moths that had a coherence above 0.6. Coherence estimates the power transfer from the input to the output and can be used as one indicator of linearity in a system. Other conditions of a linear system such as scaling and superposition need to be considered to determine the linearity of the system (Roth et al., 2011). A similar coherence cutoff has been used in moth flight system identification (Windsor et al., 2014). As experiments with wingless and abdomen-fixed moths were more challenging and had overall lower yield, presumably owing to the nature of the manipulations, we accepted moths with at least one 20-s trial with continuous flight and coherence ≥0.5. Trials in which moths could not fly continuously for 20 s were discarded.

Kinematic tracking

Two high-speed cameras (Basler acA640-120gm and Point Grey U3 03S2M) were used to track the moth head and abdomen movements separately at 100 frames s^{-1}. These two cameras were synchronized and externally triggered using a data acquisition system (National Instruments, USB-6210). A photodiode (TEMT6000 Light Sensor) mounted at the bottom of the monitor was used to synchronize the stimulus with the torque and camera signals. Specifically, the initial edge of the photodiode signal marked the start of the stimulus.

We used custom MATLAB (MathWorks) code to process the camera data and track the head and abdomen positions (Cellini et al., 2022). The head and abdominal angles were defined relative to the thorax with clockwise direction taken as positive (Fig. 1E). We first manually defined the neck joint and abdomen joint for each moth. Then, we binarized each frame such that the moth appeared white on a black background. We eroded each frame with a spherical structuring element to remove the legs and antennae. Then, we computed the radius and angle of every white pixel (part of the moth) with respect to the head and abdomen joints. We took the farthest ∼100 points from the neck joint in the upper 180 deg of each frame and computed the mean, effectively tracking the tip of the head. We then computed the angle of this point with respect to the neck joint, yielding the head angle about the yaw axis. We did the same for the abdomen but took the farthest 100 points at the bottom 180 deg of each frame.

Data analysis

Data analysis was performed in MATLAB. The torque data were digitally filtered with a low-pass Butterworth filter with a cutoff frequency of 10 Hz to filter out corrupting noise near wingbeat frequency. Head and abdominal angles were not filtered. The moth responses and stimulus were evaluated in the frequency domain using a discrete Fourier transform (calculated using MATLAB's *fft* function). All data were linearly detrended using the MATLAB function 'detrend' to reduce DC content. Bode plots were obtained by calculating the ratio between the output (moth response) and input (stimulus) in the complex domain. Gain was calculated for each trial using MATLAB's *abs* function and phase was calculated using the *angle* function. Gain and phase were evaluated for each moth, and we report the grand mean and standard deviation across all individuals. The mean and standard deviation of the phase were calculated using the MATLAB Circular Statistics Toolbox (Berens, 2009). We also computed the coherence between the stimulus and the moth response (see description above). From Bode plots, we estimated transfer functions using the function *tfest* in MATLAB. We determined that transfer functions with three poles and one zero were sufficient to capture the dynamics of the frequency response functions. In conjunction with complex domain analysis, these transfer functions were used to predict the wing torque from abdomen torque and total torque data.

Numerical simulation

To explore the role of the abdomen in flight control about yaw and contextualize the data from the rigid-tether system, we simulated zero angular momentum maneuvering of the thorax (thorax and head) in response to abdomen flexion using a two-link rigid body system. The use of this model was inspired by studies of tail use in jumping lizards and the full details of the derivation can be found in Libby et al. (2012). One link represented the thorax and the other represented the abdomen, and these two links were joined by a one degree-of-freedom (DOF) revolute (pin) joint. The model was derived with the absolute thorax and abdominal angles referenced to the vertical axis going through the pivot. To simplify the analysis, the origin of the reference frame was placed at the center of mass (COM) of the combined thorax–abdomen system (Libby et al., 2012). Briefly, the thorax and abdomen can be expressed as a nonlinear system:

$$\dot{\mathbf{x}} = \mathbf{f}(\mathbf{x}) + \mathbf{g}(\mathbf{x})u, \tag{1}$$

with the states $\mathbf{x} = \begin{bmatrix} \theta_t & \dot{\theta}_t & \theta_a & \dot{\theta}_a \end{bmatrix}^T$, where θ_t and θ_a are the angles of the thorax and abdomen, respectively, u is the relative input torque at the thorax–abdomen joint, and the nonlinear terms are:

$$\mathbf{f}(\mathbf{x}) = \begin{bmatrix} \dot{\theta}_t \\ \dfrac{a\dot{\theta}_t^2 - b}{d-e} \\ \dot{\theta}_a \\ \dfrac{-a\dot{\theta}_a^2 + c}{d-e} \end{bmatrix} \text{ and } \mathbf{g}(\mathbf{x}) = \begin{bmatrix} 0 \\ -\dfrac{f}{d-e} \\ 0 \\ \dfrac{g}{d-e} \end{bmatrix}, \tag{2}$$

Journal of Experimental Biology (2023) 226, jeb245063. doi:10.1242/jeb.245063

with constants (see Table 1 for definitions):

$$
\begin{aligned}
a &= \frac{1}{2} l_t^2 l_a^2 m_t^2 m_a^2 \sin[2(\theta_t - \theta_a)],\\
b &= [l_a^2 m_t m_a + I_a(m_t + m_a)] l_t l_a m_t m_a \dot{\theta}_a^2 \sin(\theta_t - \theta_a),\\
c &= [l_t^2 m_t m_a + I_t(m_t + m_a)] l_t l_a m_t m_a \dot{\theta}_t^2 \sin(\theta_t - \theta_a),\\
d &= l_t^2 l_a^2 m_t^2 m_a^2 \cos(\theta_t - \theta_a)^2,\\
e &= [l_t^2 m_t m_a + I_t(m_t + m_a)][l_a^2 m_t m_a + I_a(m_t + m_a)],\\
f &= [l_a^2 m_t m_a + I_a(m_t + m_a) - l_t l_a m_t m_a \cos(\theta_t - \theta_a)](m_t + m_a),\\
g &= [l_t^2 m_t m_a + I_t(m_t + m_a) - l_t l_a m_t m_a \cos(\theta_t - \theta_a)](m_t + m_a).
\end{aligned}
\tag{3}
$$

Hawkmoth morphometric data was borrowed from previous work (Dyhr et al., 2013; Hedrick and Daniel, 2006) (Table 1). The torque acted at the pin joint and represented the actuation at the pivot. We assumed no external torque or damping; thus, our results provide an upper bound on zero angular momentum maneuvering in flight. The model was computationally solved using the MATLAB function *ode45*. We also simulated a sinusoidal abdominal input torque of the form τ_a=0.005cos[2π(0.5)t].

RESULTS

Head, wing and abdomen coordination during yaw turns

We stimulated the yaw optomotor reflex by presenting tethered moths with a sum-of-sines visual stimulus. We measured the head and abdomen angles as well as the total yaw torque in response to the stimulus (Fig. 1F; Movie 1). The head response and torque were in phase with the stimulus, and we confirmed that the abdomen response was out of phase with the stimulus, according to our clockwise-positive global coordinate system (Fig. 1E,F) (Parthasarathy and Willis, 2018). The torque measured at the sensor (τ_{tot}) is the sum of the torque due to flapping wings (τ_w) and torque due to abdominal flexion (τ_a) (Fig. 2A,B). As the sensor was located near the center of pressure of the wings, it registered the approximate torque applied by the wings. Abdomen movement could generate a torque at the sensor as well, which could constructively or destructively add to the wing torque. As the head has a small mass relative to that of the thorax and abdomen – ∼5% of the total mass (Dyhr et al., 2013) – we assumed its contribution to the total torque to be negligible.

Time- and frequency-domain analysis revealed that the total yaw torque and head response resembled a high-pass filter, as evidenced by the increase in gain with increasing frequency and the positive phase at lower frequencies (Fig. 2C,D). Here, gain is defined as the ratio between the output response and the input stimulus, and phase is the difference in timing between the output and the input. Yaw torque, abdomen and head angles were overall highly coherent with the stimulus, suggestive of a linear power transfer between input and output.

Table 1. Model parameters for simulation of the thorax and abdomen of *Manduca sexta*

Parameter	Symbol	Value
Mass of the thorax (kg)	m_t	0.726×10^{-3}
Mass of the abdomen (kg)	m_a	0.999×10^{-3}
Length of the thorax (m)	l_t	12×10^{-3}
Length of the abdomen (m)	l_a	30.6×10^{-3}
Moment of inertia of the thorax (kg m^2)	I_t	1.8×10^{-7}
Moment of inertia of the abdomen (kg m^2)	I_a	3.9×10^{-7}

The abdomen regulates total flight torque

How did the abdomen and wing torque contribute to the total torque production? With the tether attached to the thorax, the sensor measured external torque from the whole moth, which originates from the wings and abdomen and is expressed as $\tau_{tot} = \tau_w + \tau_a$, where τ_{tot} is the total torque, τ_w is the torque produced by wings, and τ_a is the torque produced by the abdomen. To resolve the role of the abdomen, we first isolated τ_a by ablating both wings (Movie 2). Because the wings were removed, we assumed that the abdomen torque τ_a would be the dominant external torque (Fig. 3A). We verified that wing ablation did not significantly alter the abdominal response by comparing abdomen angles between intact and wingless moths (Fig. S2A,B), thus providing some assurance that wing ablation does not fundamentally alter abdominal responses. Despite similarities, we observed that wingless abdominal torque data were considerably noisier (Fig. 3A), perhaps owing to movement of the wing bases and changes in wing–thorax mechanics (Movie 2). Nevertheless, the abdomen torque response had distinct peaks at our stimulus frequency with high signal-to-noise ratio (Fig. S2C). With the abdominal torque and total torque known, we predicted the torque produced by the wings in response to our visual stimulus as $\hat{\tau}_w = \tau_{tot} - \tau_a$, assuming linearity (Fig. 3C). To account for the phase differences, the predicted wing torque was calculated in the complex domain. From this linear model, we predicted that the wings produced a larger torque than that produced by the abdomen at all frequencies (Fig. 3D,E). This prediction was not sensitive to whether we computed the predicted wing torque $\hat{\tau}_w$ using the complex domain or using a transfer function (Fig. S2D). To verify our prediction, we quantified the actual wing torque τ_w by measuring the torques of moths with a fixed abdomen, thus isolating wing torque (Fig. 3B). The striking similarities between $\hat{\tau}_w$ and τ_w suggest that a linear model is sufficient to capture the interaction between wing and abdomen torques on total torque generation.

To determine the interactions between the abdomen and wings on total torque generation, we computed the percentage contribution of the abdomen as $(G_a/G_w)\times100$, where G_a is the abdominal gain and G_w is the wing gain. The ratio of abdomen gain to wing gain was lower than 50% at low frequencies, but as much as 80% at the highest frequency, suggesting that the abdomen may be most effective at high frequencies (Fig. 3F). Collectively, these results suggest that the abdomen can influence thorax torques, particularly at higher frequencies, which is consistent with its role in inertial redirection.

A numerical simulation supports the constructive role of the abdomen for yaw control

At face value, the abdomen appears to act as a brake to counteract wing torques as the abdomen and wings generate torques that are antiphase. However, the constraints of the rigid-tether system confound this interpretation. The torque phase in wingless moths reflected active rotation of the abdomen, but the abdomen torque could be transferred to rotate the thorax, as the abdomen and thorax act like a two-link system. By conservation of angular momentum, a torque would act on the thorax in the opposite direction (in phase with τ_w), assisting the steering effort of the moths. To further explore the role of abdomen flexion in flight control, we modeled the thorax and the abdomen as a planar, two-link system, thus simulating more realistic dynamics than the rigid-tether system (Fig. 4A). With the measured abdominal torque as the input, the thorax rotated 2.5 times

Journal of Experimental Biology (2023) 226, jeb245063. doi:10.1242/jeb.245063

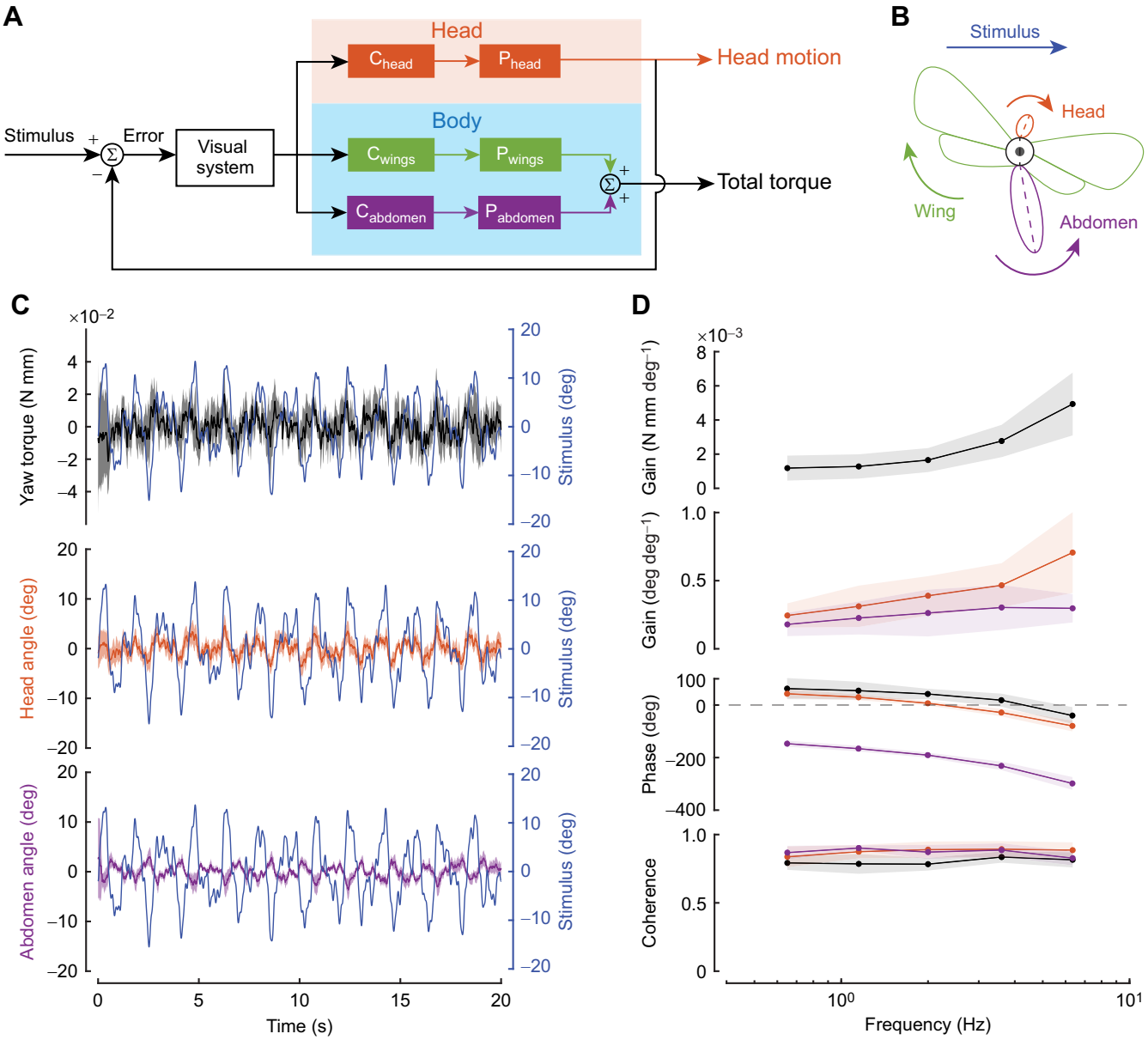

Fig. 2. Head, wing and abdomen coordination during yaw turns. (A) The control diagram hypothesizes how a tethered moth responds to a visual stimulus. The total torque consists of the wing and abdomen torques. C, controller; P, plant. (B) A visualization of the head, wing and abdominal response with respect to the stimulus direction for a tethered moth. (C) Mean yaw torque, head and abdominal responses. (D) Gain, phase and coherence for the yaw torque, head and abdominal angles. Yaw torque: n=11 moths. Head angle: n=16 moths. Abdominal angle: n=5 moths. Shaded region: ±1 s.d. Circles: mean.

as much as the abdomen owing to conservation of angular momentum (Fig. 4B), suggesting that the abdomen can amplify movement of the thorax, although this represents an upper bound as damping (external moment) was not included in our model. Importantly, our simulation showed that the thorax moved out of phase with the abdomen, suggesting that abdominal torque would constructively add to wing torque by rotating the thorax in the direction of visual motion (Fig. 2B). This conclusion was not sensitive to the type of abdominal torque input or torque amplitude and frequency (Fig. 4C; Movie 3, Fig. S3). Taken together, these results support the notion that the abdomen can significantly alter movement of the thorax, and that when considering more realistic rigid body dynamics and Newton's laws, the abdomen torque can constructively add to the wing torque.

DISCUSSION

By directly measuring flight torques of tethered moths, we discovered that the abdomen contributes significantly to wing torques about yaw. Thus, in addition to its potential role in maintaining pitch stability (Dyhr et al., 2013), the abdomen could serve to redirect the thorax inertially during free flight, thus playing a role in yaw stability and maneuverability. When considering realistic dynamics, we showed that the total torque consists of wing torque and abdominal torque and these two torques would add constructively during wide-field gaze stabilization. Our work argues for considering the role of the abdomen in tethered insect flight experiments that use torque sensors, as the abdomen can generate torques at the sensor that are as much as 80% of the wing torques at higher frequencies.

Journal of Experimental Biology (2023) 226, jeb245063. doi:10.1242/jeb.245063

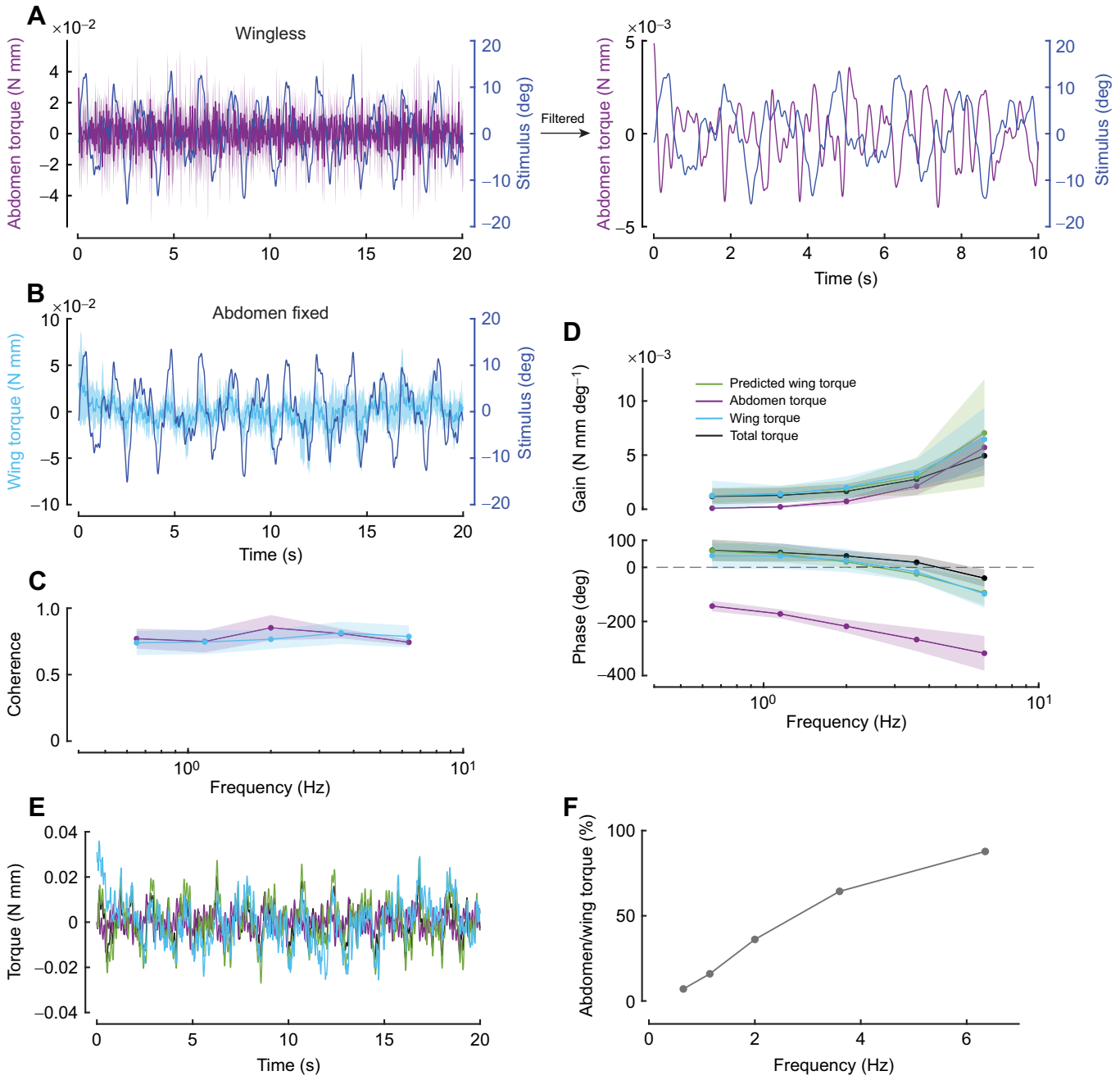

Fig. 3. The abdomen regulates total flight torque. (A) Left: yaw torque data of wingless moths in purple (low-pass filtered with 10 Hz cutoff frequency). Right: same as left but after filtering to show the antiphase response (low-pass filtered with 3 Hz cutoff frequency). Ten seconds of the 20-s trial is shown for visual clarity. Dark line: mean. *n*=4 moths. (B) Yaw torque data of abdomen-fixed moths. Dark line: mean. *n*=13 moths. (C) Stimulus–abdomen and stimulus–wing torque coherence for data shown in A and B. Solid line: mean. (D) Gain and phase of abdominal, wing (model and measured) and total torque. Solid line: mean. (E) All torques compared. The wing and abdomen torque were reconstructed by using estimated transfers functions. The key is as shown in D. (F) The contribution of the mean abdomen torque gain relative to that of the mean wing torque gain. For all panels, shaded region: ±1 s.d.

The role of the abdomen in flight control

Our results add to a growing body of evidence that the abdomen of moths can play an active role in flight control and tune wing-generated torques (Dyhr et al., 2013). By separating the abdominal torque and wing torque, we showed that the total torque is the wing torque reduced by the abdominal torque. Not surprisingly, the wing torques were larger than abdominal torque at all frequencies tested; hence, the phase of the total torque response mirrored the thorax torque phase. This result is expected as for the sum of two sine waves with the same frequency: $C\sin(\omega t+\phi)=A\sin(\omega t)+B\sin(\omega t+\delta)$, the phase ϕ is $\operatorname{atan}\frac{B\sin\delta}{A+B\cos\delta}$, thus ϕ will be dominated by the sine wave with larger amplitude (in this case, the wing-generated thorax torque). Interestingly, a linear model was sufficient to explain the interaction between wing and abdomen torques (Fig. 3D), suggesting that linear (summative) control may underlie the coordination of the abdomen and wings in flight.

Because this work was performed in tethered flight, the measured torques and angles are very likely exaggerations of actual torques and angles produced in free flight, such as when feeding from a

Journal of Experimental Biology (2023) 226, jeb245063. doi:10.1242/jeb.245063

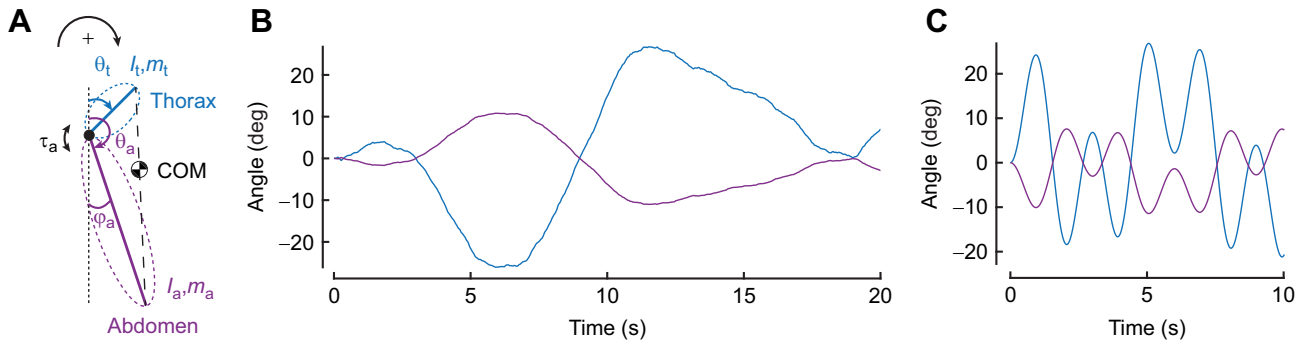

Fig. 4. A numerical simulation supports the constructive role of the abdomen for yaw control. (A) Two-degree-of-freedom, rigid-body model of the thorax and abdomen. θ_t, thorax angle; θ_a, abdomen angle; φ_a, abdomen angle relative to the vertical axis; COM, center of mass; I_t, moment of inertia of the thorax; I_a, moment of inertia of the abdomen; m_t, mass of the thorax; m_a, mass of the abdomen. (B) Simulation results. We used abdomen torque τ_a from a representative experimental trial as input. The thorax (blue) is out of phase with the abdomen angle φ_a (purple). (C) Same as B but for a sinusoidal input.

flower (Dahake et al., 2018; Sponberg et al., 2015). In free flight, the tip of the abdomen of the hawkmoth *Macroglossum stellatarum* moves by 1 mm at most (Dahake et al., 2018), whereas in our preparation, the abdomen moved by 3–5 mm. The shorter abdomen length of *M. stellatarum* (Kihlström et al., 2021) suggests that maximum abdomen angles in the rigid tether are larger than those observed in free flight in a different species (~10 deg versus ~5 deg, respectively). Interestingly, the yaw deflection magnitude of the abdomen we measured was similar to that previously measured for pitch (Dyhr et al., 2013). Further complicating the interpretation of our work, in free flight, the wings and abdomen act at the COM to modulate six DOF, whereas in our study, we effectively treated the moth as a point mass and considered a single DOF (yaw rotation). Our numerical simulation of a two-link system allowed us to contextualize the constructive role of the abdomen in flight torque generation, which was confounded by the rigid-tether system. Indeed, from the empirical torque data in the rigid tether, it would be tempting to consider that the abdomen acts as a brake. But from Newton's laws, the torque we measured in the rigid tether due to abdomen flexion acts on the thorax in an equal and opposite manner for a rotating body, as demonstrated by numerical simulation. Abdomen flexion could influence free flight dynamics in a number of ways. For example, static flexion changes the location of the COM, which can redirect wing forces, whereas dynamic flexion causes relative motion between the thorax and abdomen, as we demonstrated in the simulation (Fig. 4). Both static and dynamic flexion could influence flight dynamics and stability in subtle ways that require further investigation with more naturalistic flight physics (Berthé and Lehmann, 2015; Cheng et al., 2011). Supporting the role of the abdomen in flight control, moths with their abdomen fixed appear to have decreased flight performance (Bustamante et al., 2022). At present, although the exact way the abdomen influences the COM in free flight is not fully resolved, our results nevertheless point to an active role for the abdomen in regulating yaw torque. Another interesting possibility is that the abdomen could be used as a rudder by generating drag-induced torques. However, previous work in fruit flies showed that drag-induced torques (legs and abdomen) are about two orders of magnitude smaller than wing torques acting at the COM (Berthé and Lehmann, 2015).

Tuning of the head, thorax and abdomen

Frequency-domain analysis revealed that the total yaw torque phase is positive at low frequencies and that the gain increases with increasing frequency, indicative of a high-pass filter. Our results are broadly consistent with frequency-domain analysis of overall yaw torque in a different moth species (*Hyles lineata*), which had a relatively smaller phase advance at low frequencies and increasing gain with increasing frequency (Windsor et al., 2014). Similarly, *M. sexta* abdominal flexion about pitch acts like a high-pass filter, suggesting that the abdomen tuning measured here spans other flight axes (Dyhr et al., 2013). Thus, these two species appear to have similar optomotor responses about yaw. In a free-flight flower-tracking paradigm, moth body motion resembles a low-pass filter (Sponberg et al., 2015); however, our data show that the body torque exhibits a high-pass filter behavior. This is likely an artifact of rigidly tethering the moth, thus eliminating the role of body inertia. Furthermore, our results confirm the critical role of head movement in motion vision compensation in insect flight (Cellini and Mongeau, 2020; Cellini et al., 2022; Windsor and Taylor, 2017).

Perplexingly, the total yaw torque was slightly phase advanced relative to the head response. Due to neural conduction delays, we would expect the total yaw torque to have a phase lag instead of lead relative to the head, as shown in *Drosophila* (Cellini and Mongeau, 2020). However, one possibility is that the abdomen torque could interact with the wing torque, shifting its phase subtly. As the abdomen moved in the opposite direction of the stimulus, we interpreted this as a negative phase (a positive phase means that the moth would act on the stimulus a full cycle ahead). This antiphase behavior is similar to what has been observed in flies and locusts (Camhi, 1970b; Zanker, 1988). The notion that the abdomen has increased gain at higher frequencies is consistent with the role of the abdomen to redirect inertial forces, which are proportional to acceleration. Rapid acceleration (and velocity) of the abdomen could be used to quickly reorient the thorax in flight during rapid aerial maneuvers (Cheng et al., 2011). Indeed, the effectiveness of body parts such as tails in redirecting the body via zero angular momentum maneuvering is proportional to the ratio of their inertias (Johnson et al., 2012).

Inspiration for robotics

Actuated appendages such as tails can be very effective at redirecting inertial forces (Libby et al., 2016). The moth abdomen has already served as inspiration for the design of biologically inspired control for flying robots (Demir et al., 2012; Singh et al., 2019). Although the focus has been on stabilizing pitch (Dyhr et al., 2013), which is an inherently unstable axis in flight (Taylor and

Thomas, 2003), our work argues that appendage inertia could also be used about other axes in flight to redirect the body.

Acknowledgements
We thank undergraduate Kaitlyn Rossi for experimental assistance and maintaining the moth colony. We thank Bo Cheng for valuable comments.

Competing interests
The authors declare no competing or financial interests.

Author contributions
Conceptualization: V.L., R.J.S., J.-M.M.; Methodology: V.L., R.J.S., J.-M.M.; Software: V.L., B.C.; Formal analysis: V.L., B.C.; Investigation: V.L.; Resources: R.J.S.; Data curation: V.L.; Writing - original draft: V.L., J.-M.M.; Writing - review & editing: B.C., R.J.S., J.-M.M.; Supervision: R.J.S., J.-M.M.; Project administration: R.J.S., J.-M.M.; Funding acquisition: R.J.S., J.-M.M.

Funding
This work was funded by the Huck Innovative and Transformational Seed Fund through the Huck Institutes of the Life Sciences, Pennsylvania State University to R.S. and J.-M.M., and an Alfred P. Sloan Foundation Research Fellowship (FG-2021-16388) to J.-M.M.

Data availability
All data and code are available from Penn State ScholarSphere: https://doi.org/10.26207/n8j0-tc72

References

Berens, P. (2009). CircStat: a MATLAB toolbox for circular statistics. *J. Stat. Softw.* **31**, 1-21. doi:10.18637/jss.v031.i10
Berthé, R. and Lehmann, F.-O. (2015). Body appendages fine-tune posture and moments in freely manoeuvring fruit flies. *J. Exp. Biol.* **218**, 3295-3307. doi:10.1242/jeb.122408
Bustamante, J., Ahmed, M., Deora, T., Fabien, B. and Daniel, T. L. (2022). Abdominal movements in insect flight reshape the role of non-aerodynamic structures for flight maneuverability I: model predictive control for flower tracking. *Integr. Org. Biol.* **4**, obac039. doi:10.1093/iob/obac039
Camhi, J. M. (1970a). Sensory control of abdomen posture in flying locusts. *J. Exp. Biol.* **52**, 533-537. doi:10.1242/jeb.52.3.533
Camhi, J. M. (1970b). Yaw-correcting postural changes in locusts. *J. Exp. Biol.* **52**, 519-531. doi:10.1242/jeb.52.3.519
Cellini, B. and Mongeau, J.-M. (2020). Active vision shapes and coordinates flight motor responses in flies. *Proc. Natl. Acad. Sci. USA* **117**, 23085-23095. doi:10.1073/pnas.1920846117
Cellini, B., Salem, W. and Mongeau, J.-M. (2022). Complementary feedback control enables effective gaze stabilization in animals. *Proc. Natl. Acad. Sci. USA* **119**, e2121660119. doi:10.1073/pnas.2121660119
Cheng, B., Deng, X. and Hedrick, T. L. (2011). The mechanics and control of pitching manoeuvres in a freely flying hawkmoth (*Manduca sexta*). *J. Exp. Biol.* **214**, 4092-4106. doi:10.1242/jeb.062760
Dahake, A., Stöckl, A. L., Foster, J. J., Sane, S. P. and Kelber, A. (2018). The roles of vision and antennal mechanoreception in hawkmoth flight control. *Elife* **7**, e37606. doi:10.7554/eLife.37606
Demir, A., Ankarali, M. M., Dyhr, J. P., Morgansen, K. A., Daniel, T. L. and Cowan, N. J. (2012). Inertial redirection of thrust forces for flight stabilization. In *Adaptive Mobile Robotics* (ed. A. K. M. Azad, N. J. Cowan, M. Osman Tokhis), pp. 239-246. World Scientific Publishing Company.
Dyhr, J. P., Morgansen, K. A., Daniel, T. L. and Cowan, N. J. (2013). Flexible strategies for flight control: an active role for the abdomen. *J. Exp. Biol.* **216**, 1523-1536. doi:10.1242/jeb.077644
Eckert, H. (1980). Functional properties of the H1-neurone in the third optic Ganglion of the Blowfly,*Phaenicia*. *J. Comp. Physiol. A* **135**, 29-39. doi:10.1007/BF00660179
Fukushima, T., Siddall, R., Schwab, F., Toussaint, S. L. D., Byrnes, G., Nyakatura, J. A. and Jusufi, A. (2021). Inertial tail effects during righting of squirrels in unexpected falls: from behavior to robotics. *Integr. Comp. Biol.* **61**, 589-602. doi:10.1093/icb/icab023
Götz, K. G., Hengstenberg, B. and Biesinger, R. (1979). Optomotor control of wing beat and body posture in drosophila. *Biol. Cybern.* **35**, 101-112. doi:10.1007/BF00337435
Hassenstein, B. and Reichardt, W. (1956). Systemtheoretische Analyse der Zeit-, Reihenfolgen- und Vorzeichenauswertung bei der Bewegungsperzeption des Rüsselkäfers Chlorophanus. *Z. Naturforsch. B* **11**, 513-524. doi:10.1515/znb-1956-9-1004
Hedrick, T. L. and Daniel, T. L. (2006). Flight control in the hawkmoth *Manduca sexta*: the inverse problem of hovering. *J. Exp. Biol.* **209**, 3114-3130. doi:10.1242/jeb.02363
Hinterwirth, A. J. and Daniel, T. L. (2010). Antennae in the hawkmoth *Manduca sexta* (Lepidoptera, Sphingidae) mediate abdominal flexion in response to mechanical stimuli. *J. Comp. Physiol. A Neuroethol. Sensory, Neural, Behav. Physiol.* **196**, 947-956. doi:10.1007/s00359-010-0578-5
Johnson, A. M., Libby, T., Chang-Siu, E., Tomizuka, M., Full, R. J. and Koditschek, D. E. (2012). Tail assisted dynamic self righting. In *Adaptive Mobile Robotics* (ed. A. K. M. Azad, N. J. Cowan, M. Osman Tokhis), pp. 611-620. World Scientific Publishing Company.
Jusufi, A., Goldman, D. I., Revzen, S. and Full, R. J. (2008). Active tails enhance arboreal acrobatics in geckos. *Proc. Natl. Acad. Sci. USA* **105**, 4215-4219. doi:10.1073/pnas.0711944105
Kihlström, K., Aiello, B., Warrant, E., Sponberg, S. and Stöckl, A. (2021). Wing damage affects flight kinematics but not flower tracking performance in hummingbird hawkmoths. *J. Exp. Biol.* **224**, jeb236240. doi:10.1242/jeb.236240
Li, Y., Cao, F., Vo Doan, T. T. and Sato, H. (2017). Role of outstretched fore legs of flying beetles revealed and demonstrated by remote leg stimulation in free flight. *J. Exp. Biol.* **220**, 3499-3507. doi:10.1242/jeb.159376
Libby, T., Moore, T. Y., Chang-Siu, E., Li, D., Cohen, D. J., Jusufi, A. and Full, R. J. (2012). Tail-assisted pitch control in lizards, robots and dinosaurs. *Nature* **481**, 181-184. doi:10.1038/nature10710
Libby, T., Johnson, A. M., Chang-Siu, E., Full, R. J. and Koditschek, D. E. (2016). Comparative design, scaling, and control of appendages for inertial reorientation. *IEEE Trans. Robot.* **32**, 1380-1398. doi:10.1109/TRO.2016.2597316
Parthasarathy, K. and Willis, M. A. (2018). Parameters of motion vision in low light in the hawkmoth *Manduca sexta*. *J. Exp. Biol.* **221**, jeb173344. doi:10.1242/jeb.173344
Roth, E., Zhuang, K., Stamper, S. A., Fortune, E. S. and Cowan, N. J. (2011). Stimulus predictability mediates a switch in locomotor smooth pursuit performance for *Eigenmannia virescens*. *J. Exp. Biol.* **214**, 1170-1180. doi:10.1242/jeb.048124
Sane, S. P. (2003). The aerodynamics of insect flight. *J. Exp. Biol.* **206**, 4191-4208. doi:10.1242/jeb.00663
Shield, S., Jericevich, R., Patel, A. and Jusufi, A. (2021). Tails, flails, and sails: how appendages improve terrestrial maneuverability by improving stability. *Integr. Comp. Biol.* **61**, 506-520. doi:10.1093/icb/icab108
Singh, A., Libby, T. and Fuller, S. B. (2019). Rapid inertial reorientation of an aerial insect-sized robot using a piezo-actuated tail. In 2019 International Conference on Robotics and Automation (ICRA), pp. 4154-4160. IEEE. doi:10.1109/ICRA.2019.8793948
Sponberg, S., Dyhr, J. P., Hall, R. W. and Daniel, T. L. (2015). Luminance-dependent visual processing enables moth flight in low light. *Science* **348**, 1245-1248. doi:10.1126/science.aaa3042
Taylor, G. K. and Thomas, A. L. R. (2003). Dynamic flight stability in the desert locust *Schistocerca gregaria*. *J. Exp. Biol.* **206**, 2803-2829. doi:10.1242/jeb.00501
Theobald, J. C., Warrant, E. J. and O'Carroll, D. C. (2010). Wide-field motion tuning in nocturnal hawkmoths. *Proc. Biol. Sci.* **277**, 853-860. doi:10.1098/rspb.2009.1677
Windsor, S. P. and Taylor, G. K. (2017). Head movements quadruple the range of speeds encoded by the insect motion vision system in hawkmoths. *Proc. R. Soc. B Biol. Sci.* **284**, 20171622. doi:10.1098/rspb.2017.1622
Windsor, S. P., Bomphrey, R. J. and Taylor, G. K. (2014). Vision-based flight control in the hawkmoth *Hyles lineata*. *J. R. Soc. Interface* **11**, 20130921. doi:10.1098/rsif.2013.0921
Zanker, J. M. (1988). How does lateral abdomen deflection contribute to flight control of *Drosophila melanogaster*? *J. Comp. Physiol. A* **162**, 581-588. doi:10.1007/BF01342633